

# Proton conductivity of new type medium-temperature proton exchange membranes

Sergey A. Stelmakh<sup>1</sup> · Alexander E. Ukshe<sup>2</sup> · Dmitriy M. Mognonov<sup>1</sup> ·  
Ksenia S. Novikova<sup>2,3</sup> · Mariya N. Grigor'eva<sup>1</sup> · Ruslan R. Kayumov<sup>2</sup> ·  
Sergey A. Bal'zhinov<sup>4</sup> · Yury A. Dobrovolsky<sup>2,5</sup>

Received: 13 January 2016 / Revised: 12 April 2016 / Accepted: 18 April 2016 / Published online: 14 May 2016  
© Springer-Verlag Berlin Heidelberg 2016

**Keywords** High temperature polymer membrane fuel cell · Proton conductivity · Composite membranes · Polyhexamethyleneguanidine · Phenylone

## Introduction

Among polymer fuel cells (FC), there is a class of devices where phosphoric acid is used as electrolyte. The retention of acid in a polymer matrix is provided by binding a part of its molecules with basic groups of the polymer. Operating temperature for such medium-temperature FC can attain 150 °C due to high thermal stability and relatively high proton conductivity at low humidity [1]. Increased operating temperature of such FC provides many advantages as compared with low-temperature FC with solid polymer membranes, among which increased tolerance of catalytic materials to CO poisoning is one of the most important parameters. Moreover, high

temperature facilitates the organization of water management in the fuel cell: the water does not condense in the liquid phase, and there is no danger of flooding of electrode pores during operation. Thus, CO-enriched hydrogen produced by the reforming of natural gas, other hydrocarbon feedstocks, and alcohols can be used for their work [2, 3].

Nowadays, the most developed polymer electrolyte membranes for medium temperature FC are based on various condensation polymers, composite materials, polymers with nitrogen-containing heterocycles, and complexes of polymers with acids [4]. For medium- and high-temperature FC, the most studied proton conductive membranes are those based on polybenzimidazole (PBI) and its derivatives doped by phosphoric acid [5, 6]. Such membranes show high thermal stability and proton conductivity in the absence of water. However, the major drawback of these materials is associated with acid leaching [7]. Condensation of water vapor formed by the FC operation, for example, by stopping and cooling the battery, leads to phosphoric acid leaching from the electrolyte and its degradation, and penetration of acid on the structural elements leads to corrosion of the latter [8–10]. Thus, the search for new polymer materials that can safely hold the acid anion is one of the important tasks of developing medium-temperature FC.

This work reports on the analysis of physicochemical properties including proton conductivity of a new class of composite proton exchange membranes based on N-phenyl-substituted polyhexamethylene guanidine (PHMG) and poly-m-phenylene isophthalamide (phenylone) doped with phosphoric acid (PHMGP-PA) at different temperatures and environmental humidity. The presence of a strong ionic bond between protonated PHMGP and phosphoric acid anions allowed one to expect that the composite material is capable to retain phosphoric acid even in conditions of high humidity and temperature.

✉ Alexander E. Ukshe  
ukshe@mail.ru

<sup>1</sup> The Baikal Institute of Nature Management, Siberian Branch of the Russian Academy of Sciences, 670047 Ulan-Ude, Russia

<sup>2</sup> Institute of Problems of Chemical Physics, The Russian Academy of Sciences, Akad Semenova av.1, Chernogolovka, Moscow region 142432, Russia

<sup>3</sup> Federal State Budget Educational Institution of Higher Professional Education “South Russian State Technical University (Novocherkassk polytechnic institute)”, 346428 Novocherkassk, Russia

<sup>4</sup> Institute of Physical Material Science, Siberian Branch, The Russian Academy of Sciences, 670047 Ulan-Ude Sakhyanovoy str., 8, Russia

<sup>5</sup> Lomonosov Moscow State University, Moscow 119991, Russia

## Materials and methods

### Materials and synthesis

Hexamethylenediamine was purified by distillation at 205 °C. *N,N'*-diphenyl guanidine was purified by recrystallization from ethanol. PHMG with the coefficient of viscosity  $\eta = 20 \text{ cm}^3/\text{g}$  was synthesized by melt polycondensation of *N,N'*-diphenylguanidine and hexamethylenediamine [11] (see Scheme in Fig. 1):

Phenylone  $[-\text{HNC}_6\text{H}_4\text{NHOCC}_6\text{H}_4\text{CO}-]_n$  was purchased from Vladimir chemical factory (Russia) with  $M_V = 30 \text{ kDa}$ . The use of phenylone as a second component of the polymer-polymer composite provides satisfactory physical and mechanical characteristics of film materials. Phenylone content in the PHMGP sample was 50 wt%. Films were formed from 10 % solution in DMF by casting on a glass substrate followed by removing the solvent. The doping of the films was carried out by 60 % orthophosphoric acid for 5 days at room temperature followed by removing the acid from the surface and drying. The average thickness of the membranes was 55  $\mu\text{m}$ .

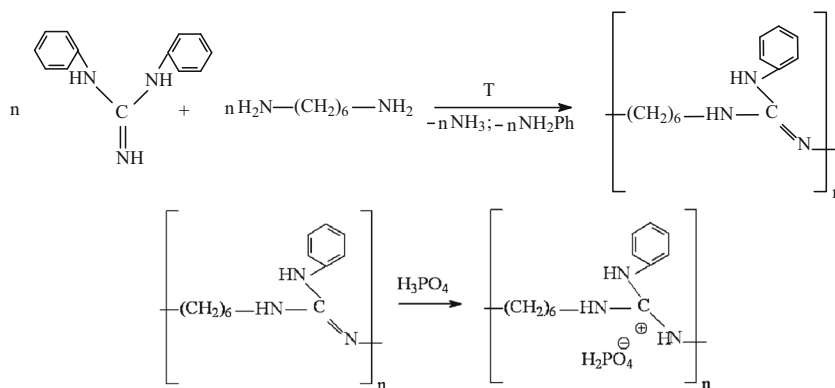
### Thermal stability

Thermal stability of the samples was determined by simultaneously by thermal analysis (STA) and mass spectrometric analysis of the decomposition products using a Netzsch STA 409 PC Luxx® instrument. The thermogravimetric analysis (TGA) and differential scanning calorimetry (DSC) curves were recorded in the 25 ÷ 1000 °C temperature range under  $\text{N}_2/\text{O}_2$  atmosphere at a heating rate of 5 °C/min.

### IR spectroscopy

The prepared samples were analyzed using IR absorption spectroscopy, IR ATR spectroscopy (a Bruker Vertex 70/70 V vacuum FTIR spectrometer with diamond ATR and RAMII module ( $\lambda_B = 1064 \text{ nm}$ ), Bruker), and the scan number was 36.

**Fig. 1** Synthetic routes to PhPGMA via polycondensation method and its doping by phosphoric acid



### Proton conductivity

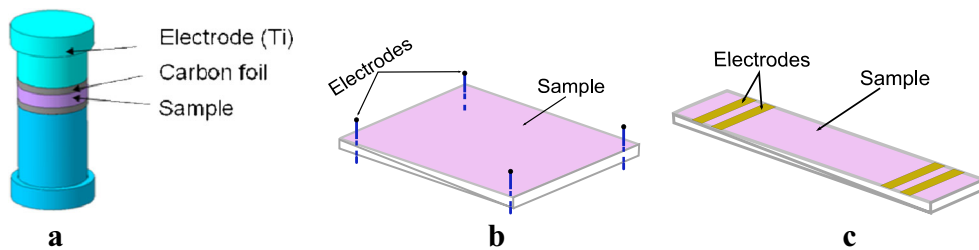
Before conductivity measurements the samples were kept in the environment of fixed humidity (not less than 2 days) at room temperature until the immutability of resistance. Saturated salt solutions were used to generate necessary pressure of water vapor. Proton conductivity AC measurements were made in two- and four-electrode cells.

In measurements using a two-electrode cell, membrane sample of 5 mm diameter was clamped between two carbon foil electrodes with pressure of about 40  $\text{kg}/\text{cm}^2$  (Fig. 2a). This arrangement of electrodes allows conductivity measurements to be performed in the direction perpendicular to the plane of the membrane. For obtaining relaxation impedance spectra Z-3000, an impedance meter (Elins, Russia) was used in the 1 Hz–3 MHz frequency range with measuring signal amplitude of 100 mV. The analysis of the frequency dependence of impedance was performed by fitting the spectra according to the equivalent circuit.

Conductivity measurements along the membrane surface were made in four-electrode cells with blocking electrodes of two types: platinum needles and gilded plates. In the first case, the measurements was carried out in a cell with electrodes (platinum needles), piercing the film at the corners of a square of 10 × 10 mm (Van der Pauw method, Fig. 2b), alternating current at 500 Hz frequency, the amplitude voltage of 6 mV, with monitoring only active component of resistance. The measurements were made using a V7–34 voltmeter (Belvar, Belarus, common mode rejection ratio of the components of more than 80 dB). The main advantage of such arrangement of electrodes is almost complete suppression of the common mode of the measured voltage that allows one to measure resistance in the direction along the membrane surface and to minimize any electrode effects.

In the second case, the sample was placed on the plate with four serial 1.3-mm-wide gilded electrodes, overlapping the entire width of the sample 5 × 33 mm (Fig. 2c) and pressed on the backside by a force of 300 N (pressure ~ 7.5 MPa) in the frequency range 1–200 kHz. The analysis of the frequency dependence of impedance measuring along the membrane

**Fig. 2** Scheme of the electrodes arrangement in the measuring cells: in the two-electrode cell (a), the Van der Pauw method (b), and the serial plates (c)



surface without the influence of the electrodes can provide information on both surface and bulk conductivity of the membrane separately.

**Results and discussion**

**Thermal stability**

When doping the film by phosphoric acid, the guanidinium groups of PHMGP have been protonated and polymer transmits to a polycationic form. This form strongly increases hydrophilicity and stabilizes the guanidinium group, whereby PHMGP resistance to hydrolysis, oxidative and thermal oxidative degradation is markedly increased.

The TGA data of the PHMGP and PHMG-PA60% membranes are shown in Fig. 3. Up to 150 °C, when no polymer destruction is observed, a single-stage dehydration process takes place, although for the doped sample, loosely water loss begins at 40 °C due to high hygroscopicity of phosphoric acid. As for the doped one and for the undoped samples, there is mass loss (8–9 %) up to 210 °C. Obviously, this mass loss corresponds to the removal of water adsorbed in the membrane. Further heating above 400 °C results in thermal degradation and combustion of the polymer (inset in Fig. 3). Complete thermal degradation of the doped sample occurs later only at temperature above 600 °C, and there is no 20 %

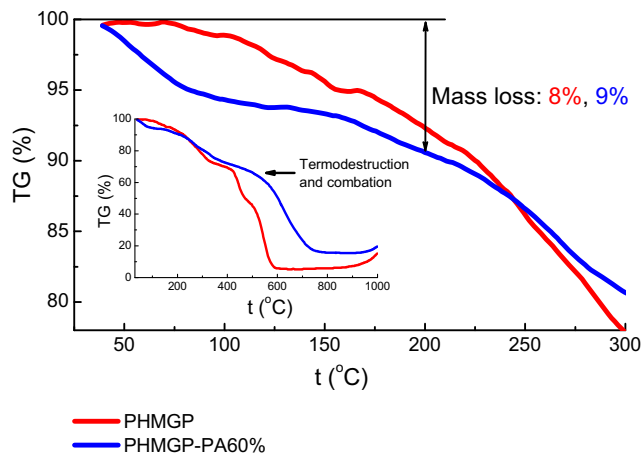


**Fig. 3** TG curves of the PHMGP and PHMGP-PA60% samples

weight loss at 450–500 °C observed on the TG curve for the undoped sample. According to the data of mass spectroscopic analysis for gas phase, the gaseous decomposition products are H<sub>2</sub>O, CO, CH<sub>2</sub>CHO, CH<sub>3</sub>CHNH<sub>3</sub>, and NH<sub>3</sub>CO.

**IR spectroscopy**

Substantial changes in the IR spectrum are observed for the membrane doped with phosphoric acid (Fig. 4). In particular, a very broad and intense absorption pick observed at 2000–3700 cm<sup>-1</sup> is characteristic of a strong hydrogen bond. In general, the spectrum is similar to the IR spectrum of the solution of phosphoric acid with characteristic absorption bands of phosphoric acid anions. Two bands with the maxima at 2336 cm<sup>-1</sup> and 2830 cm<sup>-1</sup> were found in the range of stretching vibrations of the OH group of the H<sub>2</sub>PO<sub>4</sub><sup>-</sup> anion. Their origin can be due to the Fermi resonance  $\nu(\text{OH}) \leftrightarrow 2\delta(\text{OH})$  [12–14].

**Proton conductivity**

Proton conductivity of polymer membranes can be provided by various mechanisms of proton transport in polymers. In the low-temperature polymers such as Nafion®, the transport of

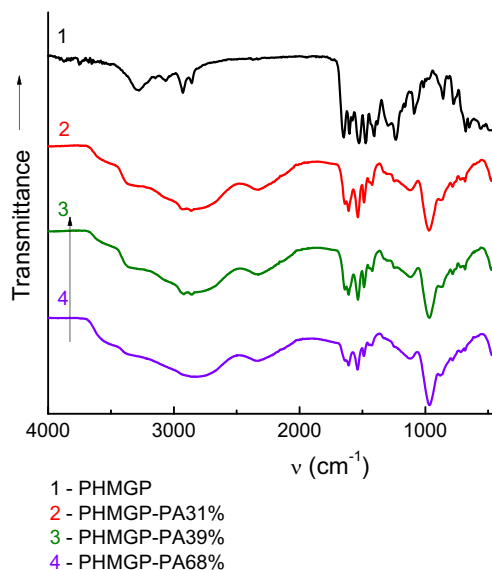


**Fig. 4** IR spectra of PHMGP (1) and PHMGP-PA (2–4)

protons in membrane occurs by the Grotthuss mechanism, wherein there is proton transfer between the water molecules bound by acidic groups of the polymer [15, 16]. Oxonium ion transport through water in the pores of the polymer is also possible. Medium-temperature membranes such as PBI conduct due to proton transport between the phosphoric acid molecules, which can hold down the minimum amount of water molecules even at high temperatures [17], i.e., the Grotthuss mechanism is realized. There is a fundamental difference between these mechanisms. In Nafion®, the  $-\text{SO}_3^-$  acid groups are a part of the polymer molecules, and thus, conductivity exists in pores and channels penetrating the bulk of the membrane. Phosphoric acid and water are labile in PBI and can be concentrated on the membrane surface not filling the pores in the bulk.

Obviously, an intermediate mechanism is realized in the studied membranes. Phosphoric acid is not included in the polymer composition but is strongly associated with it due to acid-base interaction (Fig. 1). However, less than 100 % of acid is present in the polymer as  $\text{H}_2\text{PO}_4^-$  anions. For example, at the maximal doping level (68 %), the mass of dopant (we assume that 60 % solution of  $\text{H}_3\text{PO}_4$  used for doping penetrates the membrane) is 2.125 g per 1 g of polymer. Considering that concentration of guanidine groups in the polymer is  $2.304 \cdot 10^{-3}$  mol/g, the amount of acid as bound  $\text{H}_2\text{PO}_4^-$  anions is 0.2258 g or 17.7 % of the total amount of acid. Therefore, free  $\text{H}_3\text{PO}_4$  is also present in the membrane.

Consequently, two proton transport options can be realized, namely, by liquid water, in which phosphoric acid delivers protons (in the form of oxonium ions  $\text{H}_3\text{O}^+$ ) or directly by linking with the polymer phosphoric acid by the Grotthuss mechanism.

To prove the proposed versions, proton conductivity measurements in two- and four-electrode cells were carried out. The characteristic impedance spectra of the PHMGP-PA68% membrane in the two-electrode cell are shown in Fig. 5. At low humidity, there is an additional resistive element  $R_1$  in the equivalent circuit, maybe by irregularity of dopant distribution. We accepted the sum of resistors  $R_1$  and  $R_2$  as measured resistance.

The analysis of the frequency dependence of impedance was performed by fitting the parameters of the equivalent circuit shown in inset in Fig. 5, where  $R_m = R_1 + R_2$ —resistance of the membrane, CPE1—geometrical capacitance of the cell with the membrane is  $\sim 300$  pF, C2—double layer capacitance on the electrode surfaces, W1—limited Warburg element describing diffusion relaxation of the double layer. This circuit is typical for adsorption relaxation impedance of blocking electrodes in the presence of two types of carriers [18]. The resulting resistance value is close to the value corresponding to the cut-off on the real axis obtained by extrapolating the circle arc and corresponds to a transverse bulk component of the total membrane resistance.

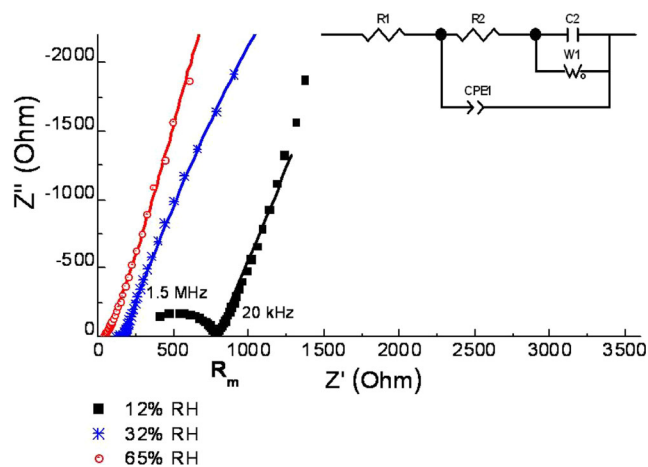


**Fig. 5** Impedance spectra of the PHMGP-PA68% membrane in the two-electrode cell (room temperature). Lines indicate extrapolation curves

The temperature dependence of transverse proton conductivity of the PHMGP-PA68% membrane has a complicated character (Fig. 6).

The temperature dependence of proton conductivity is obviously divided into three specific regions: A, B, and C.

Region A (from 20 to 60–70 °C) is close to the exponential growth of conductivity with temperature. It is area of low temperatures, and at high humidity this area, is expanded to higher temperatures. In this area, the temperature dependence of proton conductivity has Arrhenius character and increases with increasing humidity. Conductivity attains 6 mS/cm at 70–80 °C.

In region B (60–90 °C), a drop of conductivity is observed with increasing temperature (to 0.2–1.0 mS/cm at 90 °C).

In region C (over 90 °C), regrowth of proton conductivity by related acid (containing remaining strongly bound water molecules) was observed. It may be noted that there is a slowing of the loss of water at TGA in this temperature range. The value of ionic conductivity of  $10^{-3}$  S/cm at 150 °C

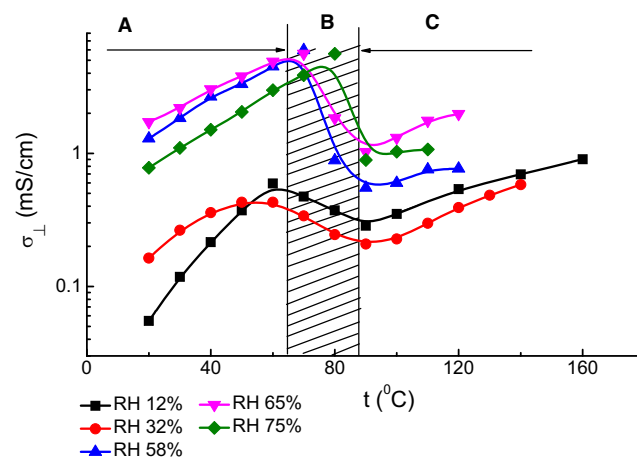


**Fig. 6** Temperature dependences of transverse proton conductivity of the PHMGP-PA68% membrane (two-electrode method)

provides the opportunity to use these membranes in the medium-temperature FC.

Reproducibility of the data upon cooling down from high temperature was verified for humidity RH = 32 %, and for RH = 10 % above 90 °C. Maximal heating at high humidity is accompanied by partial loss of water, so extra humidification is required after cooling.

The dependence of bulk conductivity on humidity at low temperatures is normal (Fig. 7): conductivity increases with increasing ambient humidity.

To measure longitudinal conductivity of the membranes, we used the Van der Pauw method. The advantage of this method consists in excluding the effect of electrodes on measurement data. The dependence of conductivity on content of phosphoric acid is complicated (Fig. 8b). At low concentration, the dependence corresponds to the percolation mechanism with the percolation threshold at  $x_c = 26$  wt% of  $H_3PO_4$  [19] (Fig. 8a). In terms of the percolation theory, the doped areas are isolated from each other with lower content of phosphoric acid and do not form continuous routes for electric current running. There is no conductivity at content of phosphoric acid lower than 26 wt%. One can expect that the dependence should have the percolation character at increasing concentration of phosphoric acid, i.e., increase with content of phosphoric acid in accordance with the power function  $\sigma = \sigma_0 \left| \frac{x-x_c}{x_c} \right|^t$ , where  $x$  is volume fraction of doped areas of the membrane and critical index  $t = 2$  (canonical index for three-dimensional medium). Though there are difficulties in determining a bulk distribution of dopant in the membrane, one can assume that volume fraction of doped areas of the membrane is proportional to concentration of  $H_3PO_4$ . It is seen in Fig. 8b that provided this assumption, a square-law growth of conductivity is really observed up to ~40 % concentration (blue curve) in accordance with the formula  $\sigma = \sigma_0 \left| \frac{w-w_c}{w_c} \right|^t$ , where  $w$  is

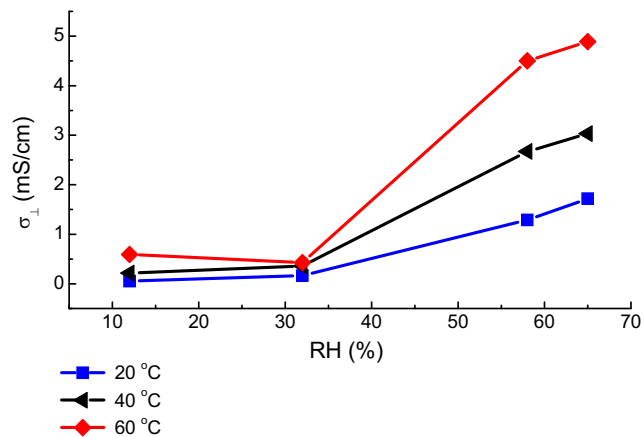


**Fig. 7** The dependence of bulk conductivity the PHMGP-PA68% membrane on humidity (region A, low temperatures)

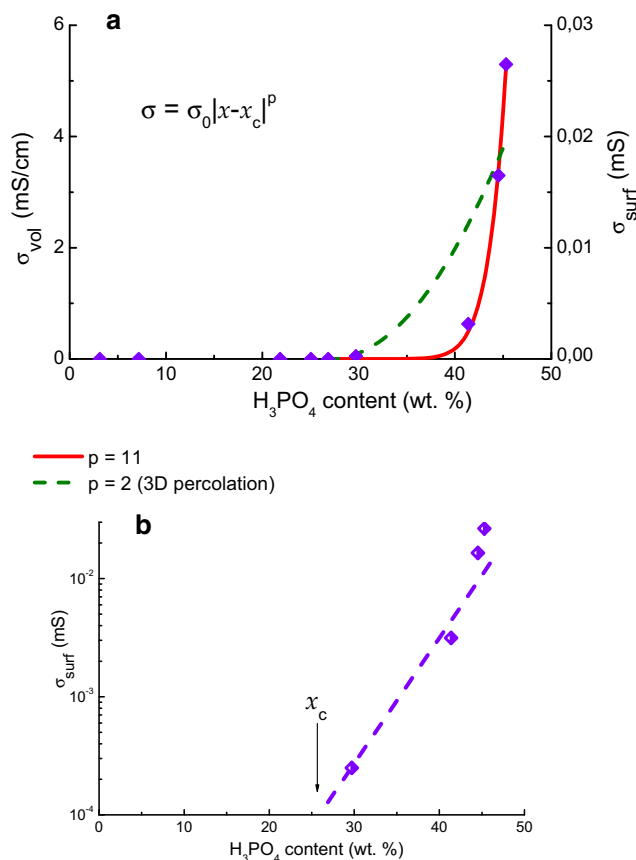


**Fig. 8** The dependence of proton conductivity on content of phosphoric acid in the PHMGP-PA membrane: **a** calculations of conductivity from the assumption of its bulk (left axis) and surface (right axis) character and **b** calculations of the percolation threshold. The Van der Pauw method, 60 % RH, 20 °C

mass concentration of phosphoric acid. However, the character of the dependence of conductivity on concentration of phosphoric acid changes at high concentrations. It is difficult to determine critical index precisely here, but it is described well by the red curve built for critical index  $t = 1.3$ , specific for surface conductivity. Seemingly, longitudinal conductivity over membrane surface plays an important role at such concentrations. No similar effects are observed in the measurements of transverse conductivity. The “crossover” effect of percolation type was also observed for thin surface layers in thin layers, for example, in [20]. Based on the assumption that surface conductivity is measured at high concentration of dopant when the Van der Pauw method is used, the values of surface conductivity were calculated from the same experimental data for concentration higher than 40 % ( $\sigma = 0.017$  mS/m for concentration of 44 % and  $\sigma = 0.027$  mS/m for concentration of 45 %).

In this regard, surface conductivity was measured for the membrane in a four-electrode cell with planar serial electrodes in the 1–10 kHz AC frequency range.

The impedance plot for the PHMGP-PA68% polymer film with four serial electrodes in the complex coordinates is shown in Fig. 9.

This spectrum is described well by a simple equivalent circuit of the  $R_1-R_2||C_1$  type (inset in Fig. 9,  $R_1 = 440$  kOhm,  $R_2 = 6.6$  kOhm). The capacitance value  $C$  parallel to resistance of the membrane at direct current (i.e., extrapolated to zero frequency) is  $630 \pm 0.9$  pF. This value of capacitance is much higher for geometric capacitance of a planar cell and much lower for a possible electrode double layer capacitance. However, this capacitance corresponds to the order of magnitude of the expected capacitance between the membrane surfaces. Therefore, we assume that conductivity of the membrane consists of two components—surface conductivity provided by the doping acid concentration on the membrane surface, and conductivity by the membrane volume. With that, two-electrode method measurements in a perpendicular direction of the membrane give a value of only bulk conductivity, and the results of measurements with a planar arrangement of electrodes contain a contribution of both bulk and high surface conductivity. Due to the impedance spectra analysis of the four-electrode data, we succeeded in separating these components. The surface conductivity magnitudes measured by the Van der Pauw method and by planar arrangement of electrodes gave similar values. However, the absolute values of conductivity are much higher (by three orders of magnitude) than those measured in the perpendicular direction of the surface. Thus, surface conductivity makes a major contribution in all four-electrode measurements (current direction along the membrane surface).

It is important to note that surface conductivity decreases with increasing ambient humidity at room temperature (Fig. 10). Obviously, this is due to the fact that in the presence of uncontrolled water sorption and desorption processes, acid-base equilibrium is established between  $H_2PO_4^-$  and  $H_2O$  and the state of associated the OH groups with the neutral acid in

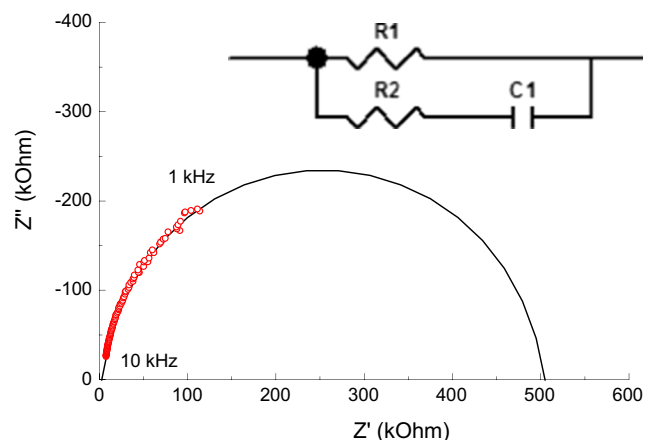


**Fig. 9** Complex plane plot of the PHMGP-PA68% membrane in a four-electrode cell with serial electrodes (room temperature). Line indicate extrapolation curve

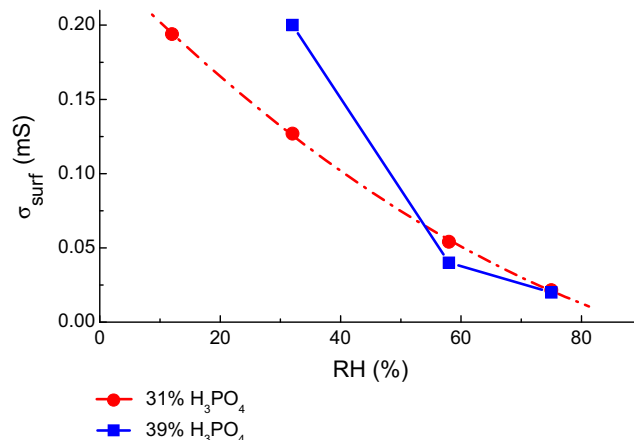


**Fig. 10** The dependence of surface conductivity of PHMGP-PA68% on relative humidity (serial electrodes)

the membrane. Excess water on the membrane surface leads to the reduction in the acid dissociation degree (reducing the concentration of mobile protons). At 100 % RH, the liquid (unbound) water may be formed on the film surface, which is manifested in some increase of surface conductivity.

Thus, proton conductivity of the PHMGP-PA membrane with a content of 68 % phosphoric acid was measured by all three methods at 75 % RH and room temperature both along and across the membrane. The value of the transverse bulk component of conductivity under these conditions was 0.78 mS/cm, while the longitudinal along the surface was 0.02 mS.

The activation energy of conductivity was calculated from the slope of the temperature dependence of conductivity in Arrhenius coordinates (Fig. 11). At RH = 10 % and, consequently, at low humidity, the conductivity activation energy is 0.5 eV, and with increasing ambient humidity, its value decreases to  $0.27 \pm 0.02$  eV and remains unchanged upon further humidification. In high-temperature region C, the activation energy is equal to the activation energy of low-temperature conductivity ( $E_a = 0.27 \pm 0.02$  eV) (Fig. 11).

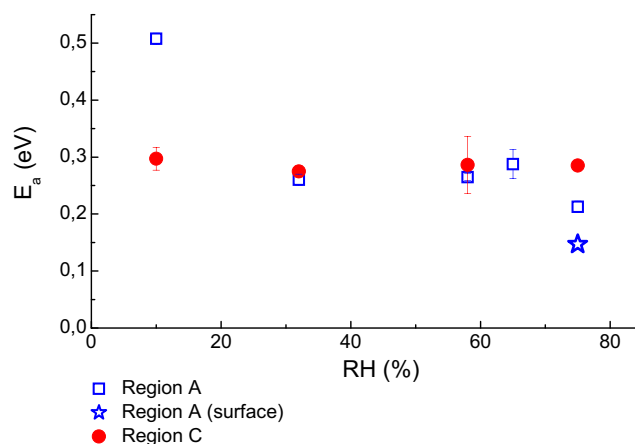


**Fig. 11** The dependence of activation energy of bulk and surface conductivity of the PHMGP-PA68% membrane on ambient humidity

The proximity of the activation energy values says in favor of the same mechanism of proton transport across the membrane and in the solution (the conductivity activation energy of phosphoric acid aqueous solutions is 0.16 eV), which is also confirmed by the presence of a developed hydrogen bonding system according to the IR spectroscopy data.

It should be noted that despite the proximity of the activation energies, the values of membrane resistances measured along and across the membranes are dramatically different. Such strong anisotropy can be related to high surface conductivity of the membrane.

The high values of surface conductivity at increased temperatures, as well as the proximity of the proton conductivity activation energy (it increases slightly to match the bulk values), says in favor of the existence of surface phosphoric acid on the membrane surface holding substantial amounts of water on the surface even at high temperatures.

The invariability of the activation energy with changing humidity and its similar values at high (above 100 °C) and low temperatures suggests that in the bulk of membrane and on its surface proton transport occurs by the same mechanism, regardless of conditions. Since at high temperatures, all loosely bound water is removed from the membrane and ion oxonium transport is unlikely, it can be assumed that all measured conductivity is governed by the Grotthuss mechanism.

## Conclusion

A method for the synthesis of new heat-resistant proton exchange membranes based on phenylone and PHMG doped by phosphoric acid operating at increased temperatures and rather firmly holding the phosphoric acid in the structure was proposed.

The existence of two types of conductivity was shown, namely, bulk proton conductivity, which attains 0.78 mS/cm at room temperature and 75 % RH, and surface conductivity along the membrane surface. A similar type of conductivity mechanism on the surface and in the bulk of the membrane was proposed.

The possibility of separation of bulk and surface conductivity of the membrane was demonstrated by impedance spectroscopy.

It was shown that the dependence of conductivity on phosphoric acid doping degree of the membrane corresponds to the percolation mechanism of formation of conducting clusters with the percolation threshold at ~25 wt%. It was found that at low temperatures (< 80 °C), the dependence of conductivity on humidity is typical for low-temperature proton exchange membranes, the activation energy decreases and conductivity increases with the hydration degree of the membranes.

Above 90 °C when usual proton exchange materials move in the non-conductive form due to water loss, effective proton

transfer with conductivity of about  $10^{-3}$  S/cm and the activation energy of  $0.27 \pm 0.09$  eV is observed.

**Acknowledgments** This work was supported by the Russian Scientific Foundation (Contract No. 14-23-00218).

**Compliance with ethical standards**

**Conflict of interests** The authors declare that they have no conflict of interest.

## References

- Dupuis AC (2011) Proton exchange membranes for fuel cells operated at medium temperatures: materials and experimental techniques. *Prog Mater Sci* 56:289–327
- Li QF, Jensen JO, Savinell RF, Bjerrum NJ (2009) High temperature proton exchange membranes based on polybenzimidazoles for fuel cells. *Prog Polym Sci* 34:449–477
- Oettel C, Rihko-Struckmann L, Sundmacher K (2012) Characterisation of the electrochemical water gas shift reactor (EWGSR) operated with hydrogen and carbon monoxide rich feed gas. *Int J Hydrog Energy* 37:11759–11771
- Park CH, Lee CH, Guiver MD, Lee YM (2011) Sulfonated hydrocarbon membranes for medium-temperature and low-humidity proton exchange membrane fuel cells (PEMFCs). *Prog Polym Sci* 36:1443–1498
- Asensio JA, Sanchez EM, Gomez-Romero P (2010) Proton-conducting membranes based on benzimidazole polymers for high-temperature PEM fuel cells. *A chemical quest Chemical Society Reviews* 39:3210–3239
- K. A. Perry, K. L. More, E. A. Payzant, R. A. Meisner, B. G. Sumpter, B. C. Benicewicz (2014) A comparative study of phosphoric acid-doped m-PBI membranes. *Journal of Polymer Science, Part B: Polymer Physics* 52: 26–35.
- Gruzd AS, Trofimchuk ES, Nikonorova NI, Nesterova EA, Meshkov IB, Gallyamov MO, Khokhlov AR (2013) Novel polyolefin/silicon dioxide/H<sub>3</sub>PO<sub>4</sub> composite membranes with spatially heterogeneous structure for phosphoric acid fuel cell. *Int J Hydrog Energy* 38:4132–4143
- Zhai YF, Zhang HM, Liu G, Hu J, Yi B (2007) Degradation study on MEA in H<sub>3</sub>PO<sub>4</sub>/PBI high-temperature PEMFC life test. *J Electrochem Soc* 154:B72–B76
- Authayanun S, Im-orb K, Arpornwichanop A (2015) A review of the development of high temperature proton exchange membrane fuel cells. *Chin J Catal* 36:473–483
- Schenk A, Grimmer C, Perchthaler M, Weinberger S, Pichler B, Heinzl C, Scheu C, Mautner FA, Bitschnau B, Hacker V (2014) Platinum–cobalt catalysts for the oxygen reduction reaction in high temperature proton exchange membrane fuel cells—long term behavior under ex-situ and in-situ conditions. *J Power Sources* 266: 313–322
- S. A. Stel'mah, L. U. Bazonov, and D. M. Mogonov (2010) On the mechanism of the hexamethylenediamine and guanidine hydrochloride polycondensation. *Russian Journal of Applied Chemistry* 83 no. 2: 342–344.
- Chapman AC, Thirlwell LE (1964) Spectra of phosphorus compounds. I. The infra-red spectra of orthophosphates. *Spectrochim Acta* 20:937–947
- Authayanun S, Mamlouk M, Arpornwichanop A (2012) Maximizing the efficiency of a HT-PEMFC system integrated with glycerol reformer. *Int J Hydrog Energy* 37:6808–6817

14. Linares JJ, Rocha TA, Zignani S, Paganin VA, Gonzalez ER (2013) Different anode catalyst for high temperature polybenzimidazole-based direct ethanol fuel cells. *Int J Hydrog Energy* 38:620–630
15. Paddison SJ (2003) Proton conduction mechanisms at low degrees of hydration in sulfonic acid-based polymer electrolyte membranes. *Annu Rev Mater Res* 33:289–319
16. Kreuer KD, Ise M, Fuchs A, Maier J (2000) Proton and water transport in nano-separated polymer membranes. *J Phys IV* 10: 279–281
17. Angioni S, Villa DC, Barco SD, Quartarone E, Righetti PP, Tomasi C, Mustarelli P (2014) Polysulfonation of PBI-based membranes for HT-PEMFCs: a possible way to maintain high proton transport at a low H<sub>3</sub>PO<sub>4</sub> doping level. *Journal of Materials Chemistry A* 2: 663–671
18. Bukun NG, Ukshe AE, Ukshe EA (1993) Frequency analysis of impedance and determination of equivalent circuit elements for solid electrolyte systems. *Russ J Electrochem* 29:100–105
19. Feder J (1988) *Fractals*. “Springer Science + Business Media, NY”, 284.
20. Clerc JP, Giraud G, Alexander S, Guyon E (1980) Conductivity of a mixture of conducting and insulating grains: dimensionality effects. *Phys Rev* 22:2489–2494